Evaluation of Magnetic Shields for Instrumented Launch Packages

S. Levinson, M. Erengil, J. Faust, and L. Burke

Institute for Advanced Technology
The University of Texas at Austin

January 2002

IAT.R 0265

Institute for Advanced Technology
The University of Texas at Austin

IAT

The views, opinions, and/or findings contained in this report are those of the author(s) and should not be construed as an official Department of the Army position, policy, or decision, unless so designated by other documentation.

REPORT DOCUMENTATION PAGE

Form Approved
OMB NO. 0704-0188

1. AGENCY USE ONLY (Leave blank)	2. REPORT DATE	3. REPORT TYPE AND DATES COVERED
	January 2002	Technical Report, 2001

4. TITLE AND SUBTITLE

Evaluation of Magnetic Shields for Instrumented Launch Packages

5. FUNDING NUMBERS

Contract # DAAD17-01-D-0001

6. AUTHOR(S)

S. Levinson, M. Erengil, J. Faust, and L. Burke

7. PERFORMING ORGANIZATION NAME(S) AND ADDRESS(ES)

Institute for Advanced Technology
The University of Texas at Austin
3925 W. Braker Lane, Suite 400
Austin, TX 78759-5316

8. PERFORMING ORGANIZATION REPORT NUMBER

IAT.R 0265

9. SPONSORING / MONITORING AGENCY NAME(S) AND ADDRESS(ES)

U.S. Army Research Laboratory
ATTN: AMSRL-WM-B
Aberdeen Proving Ground, MD 21005-5066

10. SPONSORING / MONITORING AGENCY REPORT NUMBER

11. SUPPLEMENTARY NOTES

The views, opinions, and/or findings contained in this report are those of the author(s) and should not be considered as an official Department of the Army position, policy, or decision, unless so designated by other documentation.

12a. DISTRIBUTION / AVAILABILITY STATEMENT

Approved for public release; distribution unlimited.

12b. DISTRIBUTION CODE

A

13. ABSTRACT *(Maximum 200 words)*

As part of an investigation to determine the feasibility of HSTSS telemetry techniques in EM launchers, a series of experiments was conducted to evaluate the performance of magnetic shields. The magnetic field was measured at several positions along the bore centerline of the MCL under stationary operation, and comparable EMAP3D calculations were performed. The qualitative agreement between experimental and computational results was very good. Hollow, metallic cylindrical shields were considered for their capacity to suppress the transient magnetic fields. One, comprised of Al7075, weighed 130 g; the other, of ETP Cu, weighed 430 g. The copper shield was observed to reduce the induced peak voltages by more than 80 %, which occurred at the earliest stages of the current rise. However, after 250 μs, the induced voltages were no longer attenuated by the shield. Improved shielding may be obtained with thicker or more electrically conductive cylindrical shells. If the induced fields are found to be problematic in actual EM launches, a more sophisticated shield design will be needed since the significant weight added to a 200-g launch package by this design would render its use impractical.

14. SUBJECT TERMS

Hardened Subminiature Telemetry Sensor System (HSTSS), telemetry, electromagnetic launch, magnetic shields, EMAP3D, shield design

15. NUMBER OF PAGES

21

16. PRICE CODE

17. SECURITY CLASSIFICATION OF REPORT	18. SECURITY CLASSIFICATION OF THIS PAGE	19. SECURITY CLASSIFICATION OF ABSTRACT	20. LIMITATION OF ABSTRACT
Unclassified	Unclassified	Unclassified	UL

Table of Contents

List of Figures

THIS PAGE INTENTIONALLY LEFT BLANK

Evaluation of Magnetic Shields for Instrumented Launch Packages

S. Levinson[1], M. Erengil[1], J. Faust[2], and L. Burke[2]

[1] *Institute for Advanced Technology, 3925 W. Braker Lane, Suite 400, Austin, TX 78759*
[2] *U.S. Army Research Laboratory, Aberdeen Proving Ground, MD 21005*

***Abstract*—**As part of an investigation to determine the feasibility of Hardened Subminiature Telemetry Sensor System (HSTSS) telemetry techniques in electromagnetic (EM) launchers, a series of experiments was conducted to evaluate the performance of magnetic shields. The magnetic field was measured at several positions along the bore centerline of the Medium Caliber Launcher (MCL) under stationary operation, and comparable EMAP3D calculations were performed. The qualitative agreement between experimental and computational results was very good. Hollow, metallic cylindrical shields were considered for their capacity to suppress the transient magnetic fields. One was comprised of Al7075, weighing 130 g; the other was made of ETP Cu and weighed 430 g. The copper shield was observed to reduce the induced peak voltages by more than 80% – which occurred at the earliest stages (e.g., < 100 μs) of the current rise. However, after 250 μs, the induced voltages were no longer attenuated by the shield. Improved shielding may be obtained with thicker or more electrically conductive cylindrical shells. If the induced fields are found to be problematic in actual EM launches, a more sophisticated shield design will be needed since the significant weight added to a 200-g launch package by this design would render its use impractical.

INTRODUCTION

The electronics used in the Hardened Subminiature Telemetry Sensor System (HSTSS) technology have been successfully demonstrated on conventionally launched projectiles subjected to axial accelerations as high as 75 kilogees [1]. The HSTSS technology is now being considered for electromagnetic (EM) launchers to provide on-board diagnostics for EM launched projectiles. An added concern for the HSTSS electronics used with EM launchers is the high magnetic field transients – which may render the electronics inoperable. For example, if a muzzle shunt is used with the Medium Caliber Launcher (MCL), such fields can approach 20 T at a rate of 20 T/ms at locations where such electronics are desired.

When a projectile is launched with a railgun, the voltage induced on any electronic component located in the bore is the result of two terms: one is proportional to the rate of change of magnetic flux (or rail current), and the other is proportional to the projectile velocity. While field measurements associated with a stationary armature offer only a limited approximation of comparable dynamic railgun fields, they were determined in this report to provide an order of magnitude estimate of the magnetic flux density (**B**) and the induced voltage (proportional to d**B**/dt) to which on-bore electronics will be subjected. The rail current in the full length MCL

typically rises in 500 ms to a 1.0 MA plateau, persists for a few milliseconds, and then decays to several hundred kA by the time the launch package leaves the gun. This will accelerate a 200-300 g launch package up to 2500 m/s over the first few meters of a 7-m long launcher.

Two sets of stationary experiments were conducted in order to evaluate the feasibility of HSTSS telemetry techniques in EM launchers. In the second set, which is discussed in [2], telemetry measurements using HSTSS–like electronics were analyzed in a stationary configuration of the MCL for current transients as high as 300 kA. The first set is discussed in this report, where known railgun current waveforms were used to excite measured transient magnetic flux density fields to which the HSTSS-like electronics are subjected. The experimental setup used to generate and measure these fields is discussed in the following section. The ability of metallic cylinders to mitigate the effects of the high field transients behind a fixed armature is then discussed. Finally, comparisons of the experimental measurements and corresponding analysis using EMAP3D [3] are discussed.

EXPERIMENTAL SETUP

The electric current applied to the rails and armature of the MCL, shown schematically in Fig. 1, has an associated magnetic field that is largest and perpendicular to the bore at the center. The bore and containment geometry used in this study is a typical MCL design – with 6061-T6 aluminum rails (0.75-in. x 1.75-in. cross-section) and separated 1.575 in. (40 mm) by a fixed 6061-T6 aluminum rectangular armature (1.75-in. height and 1-in. axial extension). In all measurements conducted for this report, 50-in. long rails were used.

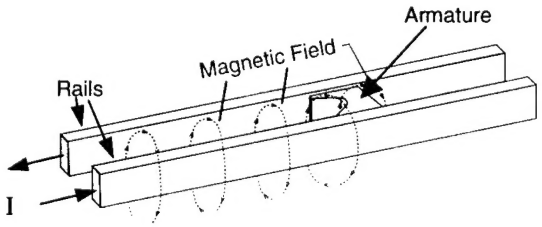

Fig. 1. A schematic diagram is shown of the armature and rails of the Medium Caliber Launcher (containment not shown). At the bore center, the magnetic flux is at its peak and is perpendicular to the bore axis.

A current waveform was used which had a linear rise proportional to that in a typical MCL launch. Virtually identical current pulses (six of which are shown in Fig. 2) were applied to the rails to produce the magnetic flux in the bore investigated in this report. The intensity of the transient magnetic field was measured with B-dot coils at different axial locations with respect to a fixed armature. Each coil was comprised of 10 turns of #26 Ga copper magnet wire, wrapped around a 0.25-in. wooden core, placed in the bore center, and oriented perpendicular to the bore axis to measure the peak component of the magnetic field. The calculated sensitivity of the coils was 3.17 V·s/T. Impedance measurements at 10 kHz of each coil were within 4 % of the value based on the calculated inductance (0.68 μH).

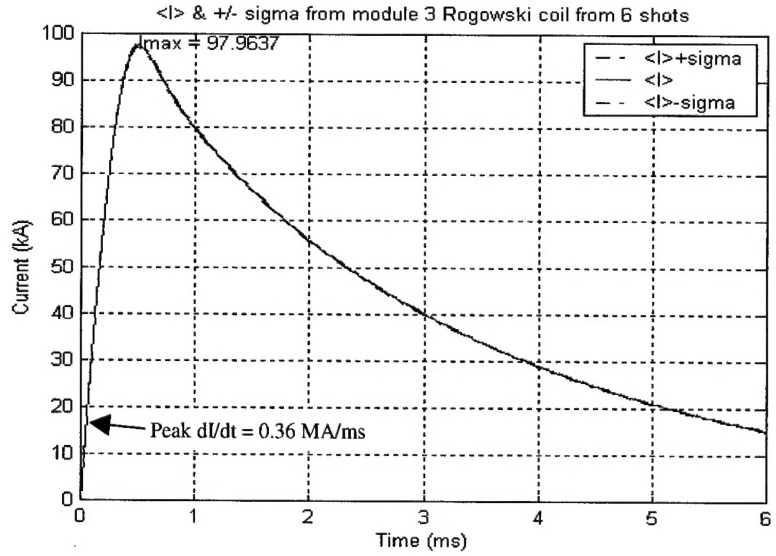

Fig. 2. Measured railgun current waveforms are shown that were used to generate the magnetic flux density **B** measured in the center of the MCL bore. For a 98 kA peak current, the peak current growth rate was 0.36 MA/ms.

The ability of a hollow, metallic cylinder to mitigate the effects of the high, transient magnetic field expected near HSTSS components was explored for each of two hollow cylindrical shields placed in the center of the bore, 2.0 in. behind the trailing edge of the armature, as illustrated in Fig. 3. Each was 6.5-in. long, with a 1.25-in. outer diameter, 0.10-in. thick wall, and closed on one end with a 0.10-in. thick wall. One shield was made of 606T6 aluminum and had a 130-g mass and electrical resistivity $\rho_e \approx 4 \cdot 10^{-8}$ Ω·m. The other was made of ETP copper, which was 3.3 times more massive and 2.4 times more conductive.

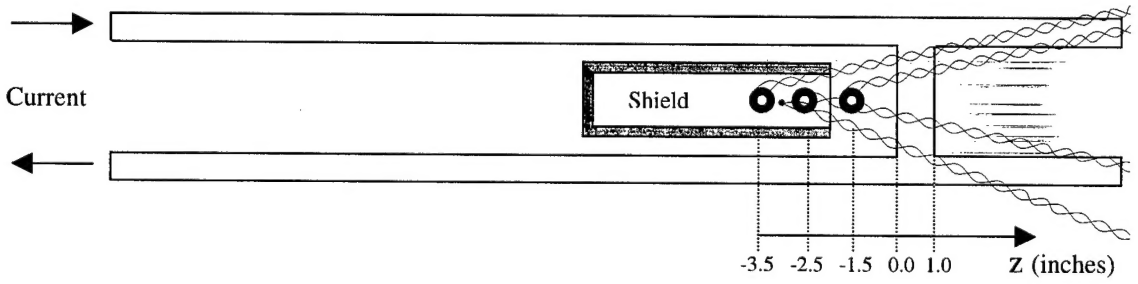

Fig. 3. Positions of the shield and field coils used to measure the magnetic field are shown relative to the armature's trailing edge; a terminated, twisted pair at -3.0 in. measured the approximate stray fields acquired by the leads of the coils. Shields were constructed of (1) air (i.e., no shield), (2) ETP copper, and (3) 6061T6 aluminum. Magnetic field measurements (with no shield) were also recorded by field coils in identical, relative position in front of the armature.

The dominant component of the magnetic flux in the MCL bore was investigated in regions where the HSTSS electronics would reside [2]. As shown schematically in Fig. 3, for magnetic

flux measurements behind the armature, two of the magnetic field coils were placed inside the shield along the centerline of the bore and shield at, respectively, 3.5 in. and 2.5 in. from the trailing edge of the armature; a third coil was placed 1.5 in. from it, outside the shield. A twisted-pair termination was also placed about 3 in. behind the trailing edge to concurrently measure the level of the stray field acquired by the 3-ft twisted-pair leads that connected each coil to 50 Ω cables, which, in turn, were connected to a digital oscilloscope to record the measurements. Magnetic field transients were also measured and recorded by the coils and terminated twisted pair leads in the same relative positions at several locations in front of the armature.

UNSHIELDED MAGNETIC FIELD MEASUREMENTS

The measured B-dot coil voltages (shown in Fig. 4) correspond to the railgun current shown in Fig. 2. They are approximately proportional to the I-dot signals provided by the Rogowski coil used to measure railgun current. However, the B-dot voltage measurements obtained behind the fixed armature (-1, -2.5, and -3.5 in.) have faster rising peaks than the I-dot measurement, and the reverse is true for corresponding measurements in front of the armature (+2.5, +3.5, and +9.5 in.).

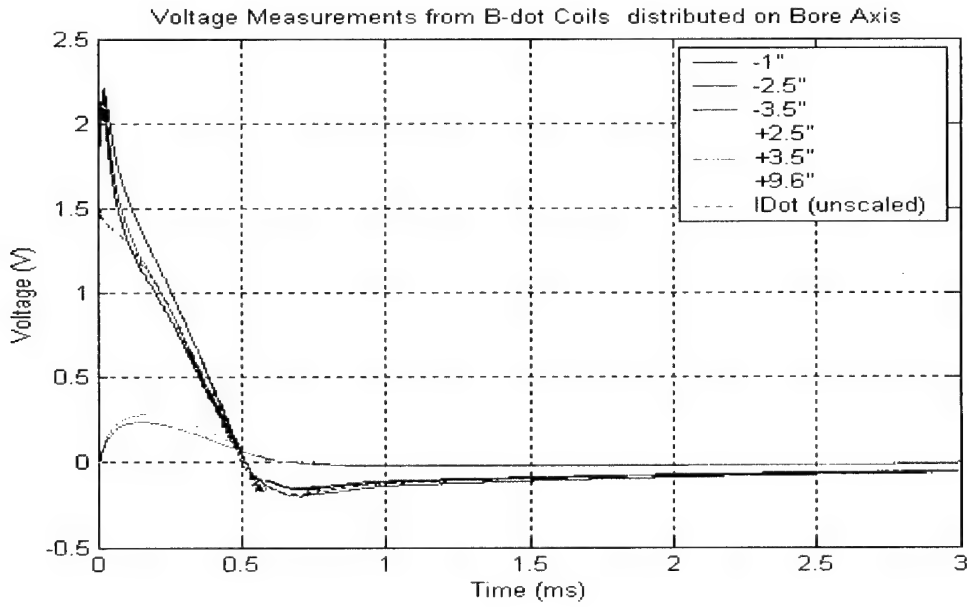

Fig. 4. B-Dot coil voltage measurements (proportional to dB_y/dt) obtained at different axial positions in the bore center are shown vs. time. Also shown are the unscaled Rogowski coil voltages used (when properly scaled and integrated) to measure the railgun current.

The B-Dot voltage measurements shown in Fig. 4 were integrated and appropriately scaled by the coil dimensions to provide estimates of the magnetic flux density **B** shown in Fig. 5. At locations behind the stationary armature, the peak amplitude of $|\mathbf{B}| \equiv B$ was 1.6 T, and the peak value of dB/dt was 6 T/ms. Here, **B** was perpendicular to the bore axis at the bore center ($\mathbf{B} \approx B\hat{\mathbf{e}}_y = B_y\hat{\mathbf{e}}_y$), approximately axially independent, and proportional to the current level at

16 T/MA. At locations past the armature, **B** was markedly reduced, measuring nearly an order of magnitude smaller at positions 2.5-3.5 in. (1.4-2 armature heights) after the trailing edge. At a location of 9.6 in. (5.5 armature heights) after the trailing edge, **B** measured more than two orders of magnitude smaller. Since, at 9.6 in., B was still larger than the stray fields acquired by the terminated twisted pair leads, it was judged a relatively noise-free, local measurement.

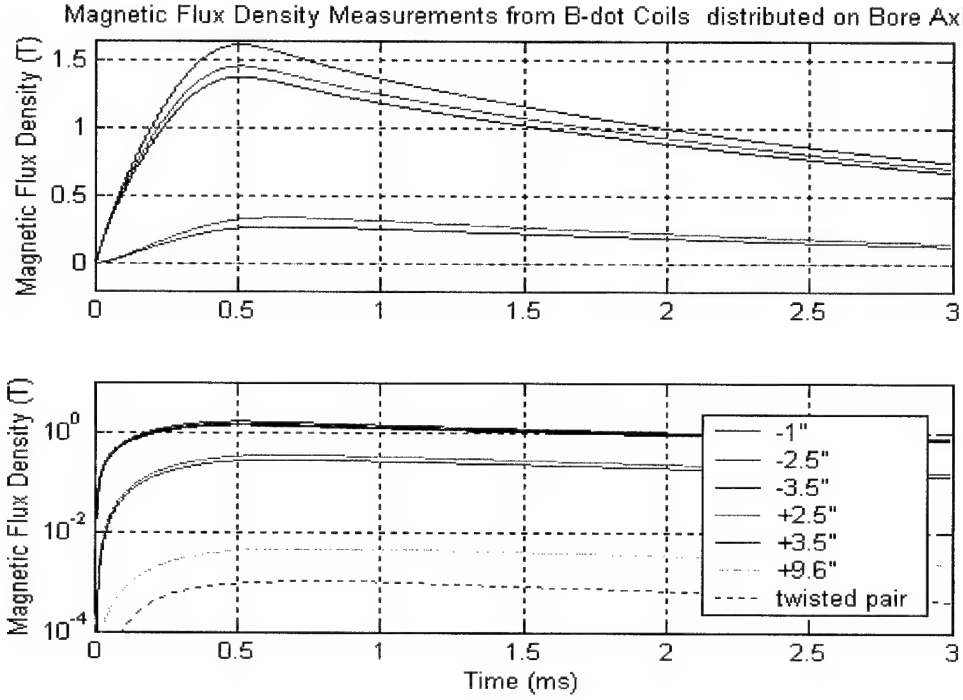

Fig. 5. Integrated and scaled values are shown of the B-Dot coil voltage measurements shown in Fig. 4 to provide estimates of the magnetic flux density (B_y). Also shown are stray fields acquired by the terminated twisted pair leads.

SHIELDED MAGNETIC FIELD MEASUREMENTS

In a railgun launch, if the armature current is not zero at exit, an electrical arc will form as the armature leaves the gun and may cause a number of undesirable consequences, most of which can be alleviated with the use of a muzzle shunt [4]. Unfortunately, when a muzzle shunt is employed, significantly larger voltage transients will develop ahead of the armature as the magnetic flux is compressed between the armature and the muzzle shunt. Transients induced because of a muzzle shunt are difficult to measure or calculate accurately. However, the muzzle voltage, normally 10-30 V on the MCL, has been measured in kilovolt ranges when such a shunt is attached, as shown in Fig. 6 [5]. Thus, the use of a muzzle shunt in an EM launcher may subject a launch package to extremely high voltage transients that could have dire consequences for on-board instrumentation, which is a principal motivation for this investigation.

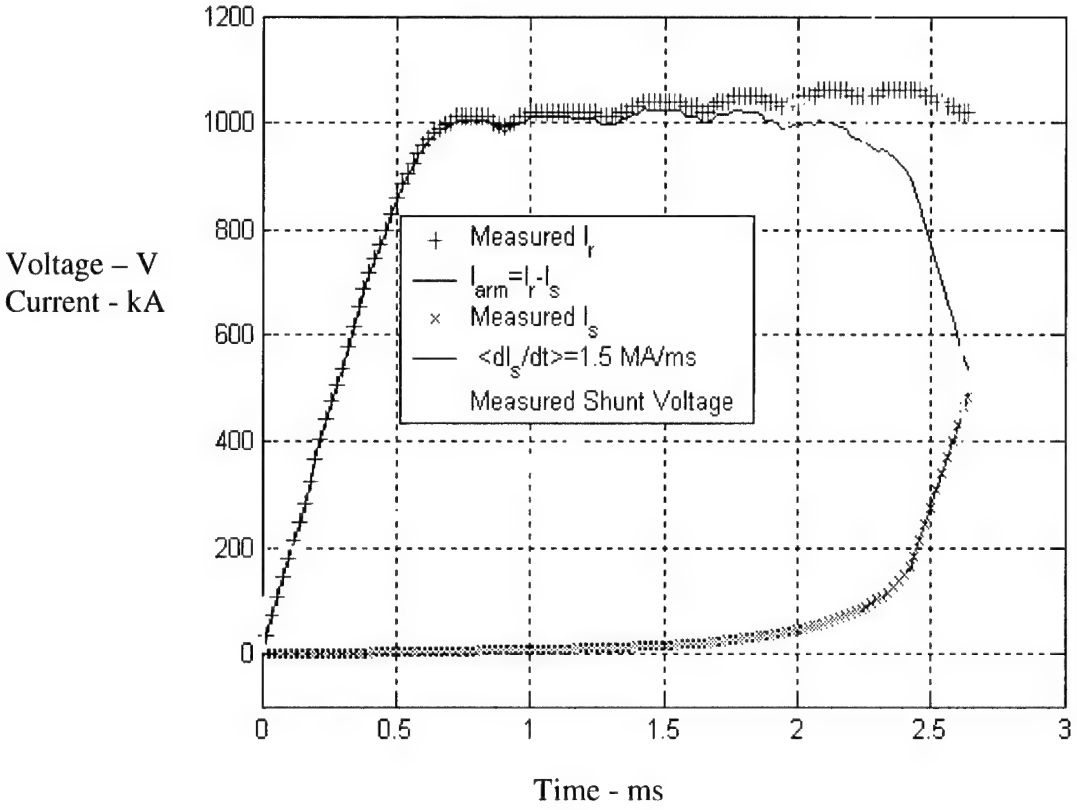

Fig. 6. Measured rail and shunt currents on the MCL are shown when a muzzle shunt is attached [5]. There is an enormous magnetic field transient in the bore associated with the sharp shunt current rise (1.5 MA/ms) at the end of the launch.

Shown in Fig. 7 (upper plot) are B-dot coil voltages measured inside aluminum and copper shields at two locations behind the armature, which correspond to the railgun current shown in Fig. 2; in the lower plot are the corresponding fractional reductions of the voltages due to the shields. The B-dot coil voltages were integrated and appropriately scaled by the coil dimensions to provide estimates of the magnetic flux density B shown in Fig. 8 (upper plot) and the corresponding fractional reductions of B due to the shields (lower plot). The greatest reduction in the magnetically induced voltage was achieved by the more conductive (and heavier) copper shield. As compared to the case with no shield, it was observed to reduce the induced peak voltages by more than 80% – which occurred at the earliest stages (e.g., < 100 μs) of the current rise. However, after 250 μs, the induced voltages were no longer attenuated by the shield. The reductions in the magnetic flux density (Fig. 8) were slightly smaller, but persisted for longer times.

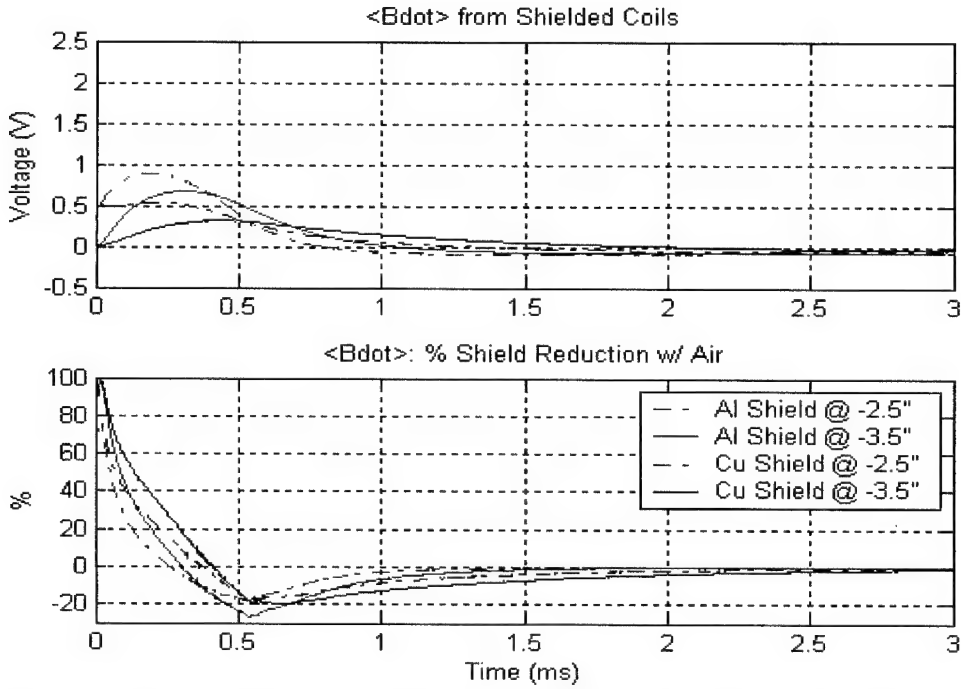

Fig. 7. Shown are induced voltages by the transient magnetic field behind the armature with shields (top) and the corresponding relative reduction by the shields (bottom):
$\{100\%*(\text{B-dot}_{\text{w/shield}} - \text{B-dot}_{\text{w/o shield}})/\text{B-dot}_{\text{w/o shield}}\}$.

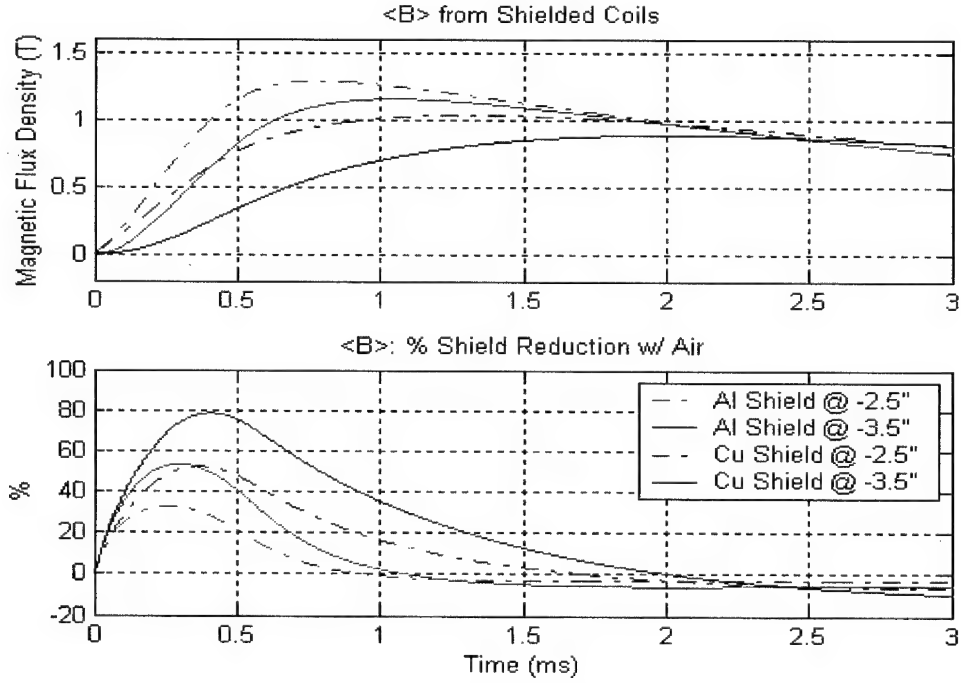

Fig. 8. Shown are magnetic flux density B behind the armature with shields (top) and corresponding relative reduction by the shields (bottom):
$\{100\%*(B_{\text{w/shield}} - B_{\text{w/o shield}})/B_{\text{w/o shield}}\}$.

COMPUTATIONAL ANALYSES

Computational analysis was performed both to corroborate with and to extrapolate from the magnetic field measurements conducted inside the magnetic shields. The 3D electromagnetic/thermal finite element code EMAP3D [3] was used to conduct a stationary analysis of the magnetic fields associated with the current profile shown in Fig. 2. Neither thermal effects nor the effects of the magnetic containment structure were included in the model. However, measurements and corresponding calculations of B are remarkably close, as shown in Figs. 9 and 10, for the employment of an aluminum shield and a copper shield, respectively. In both cases, the measured fields were as much as 0.4 T greater than corresponding calculations; however, the calculations had the same relationship as the measurements did versus time, axial position, and shield conductivity. As summarized in Fig. 11, where the three shield cases are compared during the peak current and magnetic field (at 0.5 ms), the calculations corroborate the measurements, showing the reduction in B due to the shields was greatest at the earliest times behind the armature. The calculations confirm that the copper shield provides the best early magnetic shielding of the two.

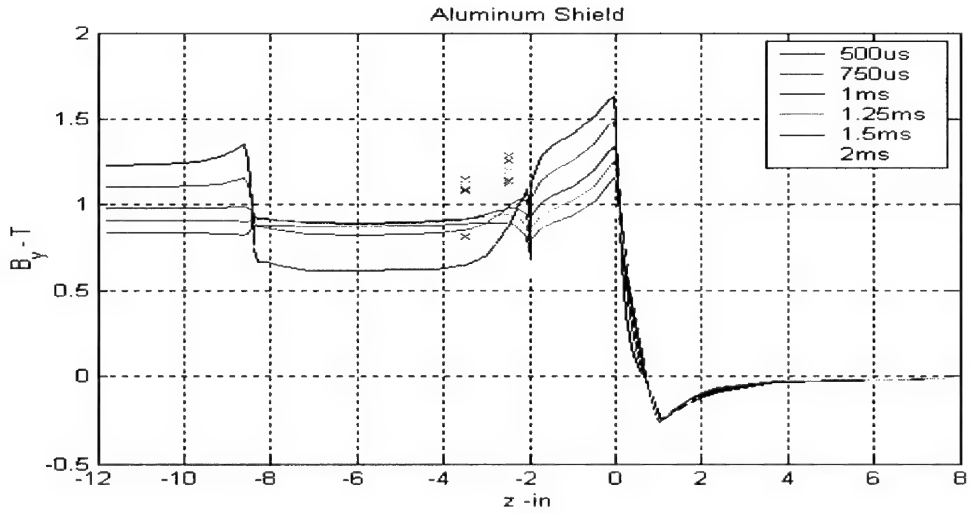

Fig. 9. Measurements (symbols) and calculations (curves) of the peak component of the magnetic flux density are shown versus axial positions in the bore for different times (see legend) with respect to the applied railgun current shown in Fig. 2. These correspond to the case of the aluminum shield occupying a region 2-8.5 in. (1-5 armature heights) behind the trailing edge of the armature.

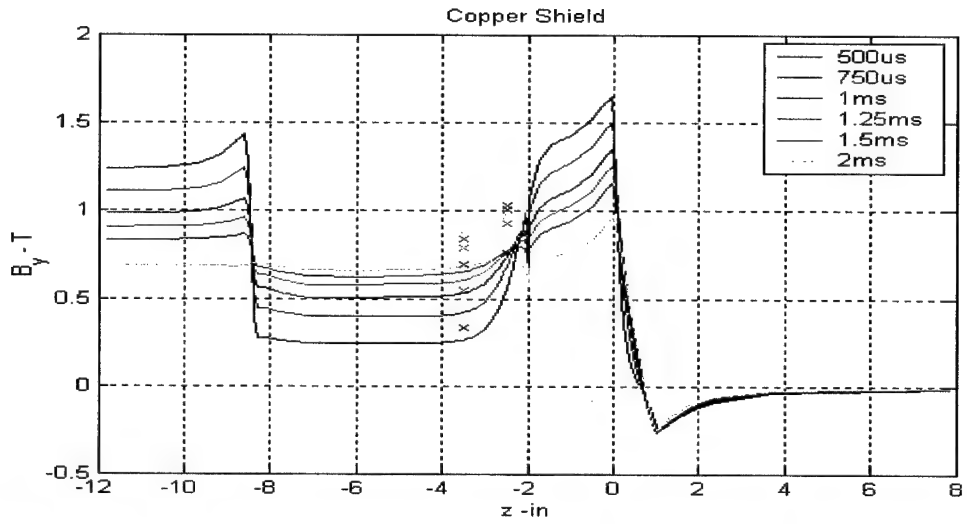

Fig. 10. Measurements (symbols) and calculations (curves) of the peak component of the magnetic flux density are shown versus axial positions in the bore for different times (see legend) with respect to the applied railgun current shown in Fig. 2. These correspond to the case of the copper shield occupying a region 2-8.5 in. (1-5 armature heights) behind the trailing edge of the armature.

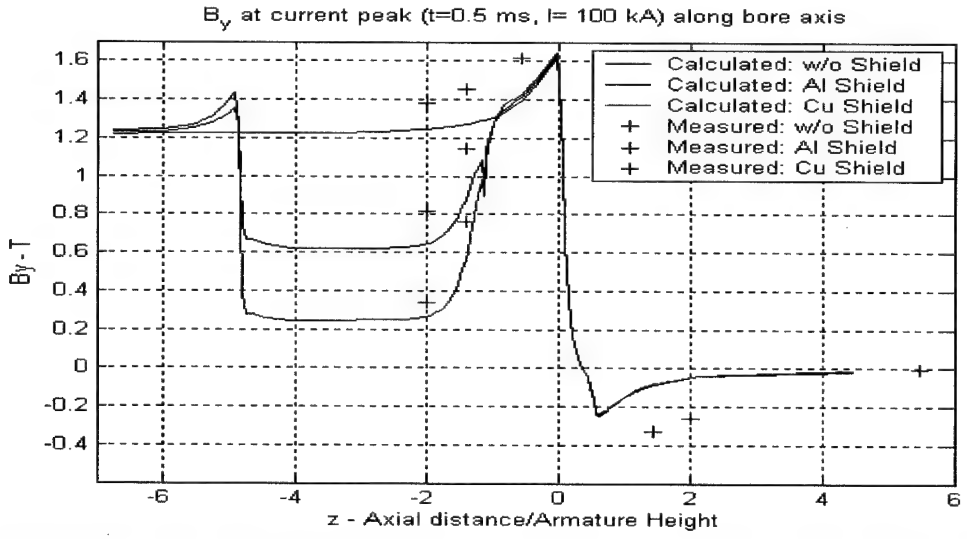

Fig. 11. Measured and calculated peak component of the magnetic flux density is shown during the current peak. The measurements and EMAP3D calculations were made for three different shield cases, which occupied a region 2-8.5 in. (1-5 armature heights) behind the trailing edge of the armature.

SUMMARY

Stationary experiments and 3D calculations using a known railgun current waveform were used to excite the magnetic flux density in the bore center. The associated magnetic field transient was calculated and measured on either side of a fixed armature in order to evaluate the rate and intensity of the transient magnetic fields to which on-board electronics would be

subjected. A proportionality factor 16 T/MA was determined between the rail current and the magnetic flux density behind the fixed armature. At locations past the fixed armature, the peak fields were markedly reduced, measuring nearly an order of magnitude smaller at axial positions 1.5-2 armature heights after the trailing edge and measuring more than two orders of magnitude smaller at positions 4.5-5 armature heights after it. Two hollow, 6.25-in. long, 0.10-in. thick cylindrical shields (closed on one end) were considered for their capacity to suppress the transient magnetic fields. One was comprised of Al7075, weighing 130 g; the other was made of ETP Cu and weighed 430 g. The greatest reduction in the magnetically induced voltage was achieved by the more conductive (but heavier) copper shield. As compared to the case with no shield, the copper shield was observed to reduce the induced peak voltages by more than 80% – which occurred at the earliest stages (< 100 μs) of the current rise. However, after 250 μs, the induced voltages were no longer attenuated by the shield. Improved shielding may be obtained with thicker or more electrically conductive cylindrical shells; however, if such shielding is found to be necessary for a particular EM launch, an improved shield design should be selected since the significant weight penalties imposed by either of these shields would render the use impractical.

ACKNOWLEDGEMENTS

The authors would like to acknowledge Mr. John Goutier of the Institute for Advanced Technology for his technical support and operation of the MCL, and Mr. Phillip Peregino and Mr. Charles Mitchell of the U.S. Army Research Laboratory for their excellent mechanical design and fabrication support. In addition, the authors would like to thank the HSTSS Project Director, Mr. Dennis Schneider, of the U.S. Army Simulation Training Instrumentation Command, for funding a significant portion of this research study.

The research reported in this document/presentation was performed in connection with Contract number DAAD17-01-D-0001 with the U.S. Army Research Laboratory. The views and conclusions contained in this document/presentation are those of the authors and should not be interpreted as presenting the official policies or position, either expressed or implied, of the U.S. Army Research Laboratory or the U.S. Government unless so designated by other authorized documents. Citation of manufacturer's or trade names does not constitute an official endorsement or approval of the use thereof. The U.S. Government is authorized to reproduce and distribute reprints for Government purposes notwithstanding any copyright notation hereon.

REFERENCES

[1] W. D'Amico, "Telemetry Systems and Electric Gun Projectiles," *IEEE Trans. Magn.* 37, January 2001, pp. 343-346.

[2] S. Levinson, L. Burke, M. Erengil, and J. Faust, "Investigating UHF Telemetry for Electromagnetic Launchers," 10th U.S. Army Gun Dynamics Symposium, Austin, Texas, April 2001 (IAT.P 0460).

[3] K. T. Hsieh, "Implementing a Tri a Tri-Potential Approach in EMAP3D," *IEEE Trans. Magn.* 35, January 1999, pp. 166-169 (IAT.P 0272).

[4] Jerald V. Parker and Scott J. Levinson, "Muzzle Arc Control Using an Inductive Shunt," *IEEE Trans. Magn.*, **33**, pp.594-598, Jan 1997 (IAT.P 0203).

[5] Private discussions with Mr. Francis Stefani and Mr. Trevor Watt, concerning muzzle shunt experiments they conducted on the MCL at the Institute for Advanced Technology (IAT) in September 2000.

THIS PAGE INTENTIONALLY LEFT BLANK

Distribution List

Defense Technical Information Center
Administrator
ATTN: DTIC-DDA
8725 John J. Kingman Road, Suite 944
Ft. Belvoir, VA 22060-6218
USA

U.S. Army Research Laboratory
Director
ATTN: AMSRL OP SD TP
2800 Powder Mill Road
Adelphi, MD 20783-1145
USA

U.S. Army TRADOC
Director
Analysis Center
ATTN: ATRC-WSS-R
White Sands Missile Range, NM 88002-5502
USA

U.S. Army Research Laboratory
Technical Library 305
ATTN: AMSRL CI LP
Aberdeen Prvg Grd, MD 21005-5066
USA

Army Research Office
P. O. Box 12211
Research Triangle Park, NC 27709-2211
USA

U.S. Army Armament Research Development and Engineering Center
Commander
ATTN: AMSTA-AR-IMC (Bldg. 30)
Picatinny Arsenal, NJ 07806-5000
USA

Benét Weapons Laboratory
U.S. Army Armament Research, Development and Engineering Center
ATTN: AMSTA-AR-CCB-TL
Watervliet, NY 12189-4050
USA

Dr. John Barber
IAP Research, Incorporated
IAP Research, Incorporated
2763 Culver Avenue
Dayton, OH 45429-3723
USA

U.S. Army Research Laboratory
Director
Attn: AMSRL OP SD TA
2800 Powder Mill Road
Adelphi, MD 20783-1145
USA

Mr. David Bauer
IAP Research, Incorporated
2763 Culver Avenue
Dayton, OH 45429-3723
USA

U.S. Army Research Laboratory
Director
ATTN: AMSRL OP SD TL
2800 Powder Mill Road
Adelphi, MD 20783-1145
USA

Dr. Bruce Burns
U.S. Army Research Laboratory
Weapons Technology Directorate
AMSRL-WT-PD, Building 390
Aberdeen Proving Ground, MD 21005-5066
USA

Distribution List

Dr. George Chryssomallis
Science Applications International Corp.
3800 West 80th Street
Suite 1090
Bloomington, MN 55431
USA

Dr. Mark Crawford
Institute for Advanced Technology (IAT)
The University of Texas at Austin
3925 W. Braker Lane, Suite 400
Austin, TX 78759-5316
USA

Mr. Daniel R. Dakin
SAIC
2000 Powell St., Ste. 1090
Emeryville, CA 94608
USA

Mike Devine
U.S. Army TACOM-ARDEC
Technical Director
ATTN: AMSTA-AR-TD
Picatinny Arsenal, NJ 07806-5000
USA

Dr. Mehmet Erengil
Institute for Advanced Technology (IAT)
The University of Texas at Austin
3925 West Braker Lane, Suite 400
Austin, TX 78759-5316
USA

Dr. Harry Fair
Institute for Advanced Technology (IAT)
The University of Texas at Austin
3925 W. Braker Lane, Suite 400
Austin, TX 78759-5316
USA

Mr. Lloyd Farris
Lockheed Martin Missiles & Fire Control
Mail Stop: WT-62
P.O. Box 650003
Dallas, TX 75265-0003
USA

Dr. Scott Fish
Defense Advanced Research Projects Agency/TTO
3701 N. Fairfax Drive
Arlington, VA 22203
USA

Dr. Bob Fossum
Institute for Advanced Technology (IAT)
The University of Texas at Austin
3925 W. Braker Lane, Suite 400
Austin, TX 78759-5316
USA

Dr. Marilyn Freeman
SAALT
Attn: SAAL-ZT
Suite 9815
2511 Jefferson Davis Highway
Arlington, VA 22202
USA

Dr. Thaddeus Gora
Consultant
4 Dogwood Trail
Kinnelon, NJ 07405
USA

Dr. Robert Guenther
U.S. Army Research Office
PO Box 12211
Research Triangle Park, NC 27709-2211
USA

Distribution List

Mr. John Gully
SAIC
1410 Springhill Rd, Suite 400
Mclean, VA 22102
USA

Mr. Gary Katulka
U.S. Army Research Laboratory
ATTN: AMSRL-WM-BA, B4600
Aberdeen Proving Ground, MD 21005-5066
USA

John Hedderick
U.S. Army Armament Research, Development and Engineering Center
Attn: AMSTA-AR-CC
Bldg. 1
Picatinny Arsenal, NJ 07806-5000
USA

Mr. Jon Kitzmiller
Center for Electromechanics
The University of Texas at Austin
PRC/EME, Mail Code R7000
Austin, TX 78712
USA

Andy Hooper
USAYPG
CSTE-DTC-YP-CD
YUMA, AZ 83685
USA

Dr. Walter LaBerge
Institute for Advanced Technology (IAT)
The University of Texas at Austin
3295 West Braker Lane, Suite 400
Austin, TX 78759-5316
USA

Mr. Albert Horst
U.S. Army Research Laboratory
Chief, Propulsion and Flight Division
ATTN: AMSRL-WT-P
Aberdeen Proving Ground, MD 21005-5066
USA

Mr. Dennis Ladd
U.S. Army ARDEC
Attn: AMSTA-AR-FSP
Picatinny Arsenal, NJ 07506-5000
USA

Kou-Ta Hsieh
Institute for Advanced Technology (IAT)
The University of Texas at Austin
3925 W. Braker Lane, Suite 400
Austin, TX 78759-5316
USA

Dr. Scott Levinson
Institute for Advanced Technology (IAT)
The University of Texas at Austin
3925 W. Braker Lane, Suite 400
Austin, TX 78759-5316
USA

Dr. Keith Jamison
Science Applications International Corporation
PO Box 4216
Fort Walton Beach, FL 32549-4216
USA

Mr. Andy Lijoi
U.S. Army TACOM-TARDEC
ATTN: AMSTA-TR-S
M.S. #207
Warren, MI 48397-5000
USA

Distribution List

David Lyon
Ballistics & Weapons Concepts
AMSRL-WM-BC
Aberdeen Proving Ground, MD 21005-5066
USA

Dr. Jerald Parker
Applied Physics Consulting
6112 Buffalo Grass Ct. NE
Albuquerque, NM 87111
USA

Dr. Hans Mark
Institute for Advanced Technology (IAT)
The University of Texas at Austin
3925 West Braker Lane, Suite 400
Austin, TX 78759-5316
USA

Dr. Chadee Persad
Institute for Advanced Technology (IAT)
The University of Texas at Austin
3925 W. Braker Lane, Suite 400
Austin, TX 78759-5316
USA

Dr. Ian McNab
Institute for Advanced Technology (IAT)
The University of Texas at Austin
3925 W. Braker Lane, Suite 400
Austin, TX 78759-5316
USA

Mr. Peter Plostins
U.S. Army Research Laboratory
ATTN: AMSRL-WM-BC
Aberdeen Proving Ground, MD 21005-5066
USA

Mr. James Newill
Weapons and Material Research Directorate
Attn: AMSRL-WM-BC
Aberdeen Proving Ground, MD 21005
USA

Dr. John Powell
Ballistic Research Laboratory
ATTN: AMSRL-WT-WD
Aberdeen Proving Ground, MD 21005-5066
USA

Dr. William Oberle
U.S. Army Research Laboratory
Weapons and Materials Research Directorat
ATTN: AMSRL-WM-BE, Building 390
4600 Deer Creek Loop
Aberdeen Proving Ground, MD 21005-5066
USA

Dr. Siddharth Pratap
Center for Electromechanics
The University of Texas at Austin
BRC, EME 133
10100 Burnet Road
Austin, TX 78758-4497
USA

Mr. John Pappas
Center for Electromechanics
The University of Texas at Austin
PRC/EME, Mail Code R7000
Austin, TX 78712
USA

Dr. Sikhanda Satapathy
Institute for Advanced Technology
The University of Texas at Austin
3925 W. Braker Lane, Suite 400
Austin, TX 78759-5316
USA

Distribution List

Mr. Robert Schlenner
U.S. Army ARDEC
Attn: AMSTA-AR-CCL-D
Building 65 N
Picatinny Arsenal, NJ 07806-5000
USA

Dr. Edward Schmidt
U.S. Army Research Laboratory
ATTN: AMSRL-WM-B
Aberdeen Proving Ground, MD 21005-5066
USA

Dennis Schneider
STRICOM
ATTN: AMSTI-ITTS-I
12350 Research Parkway
Orlando, FL 32826

Dr. Francis Stefani
Institute for Advanced Technology (IAT)
The University of Texas at Austin
3925 W. Braker Lane, Suite 400
Austin, TX 78759-5316
USA

LTC Patrick Sullivan
Institute for Advanced Technology (IAT)
The University of Texas at Austin
3925 W. Braker Lane, Suite 400
Austin, TX 78759-5316
USA

Dr. Jerome Tzeng
US ARMY Research Laboratory
WMRD
Attn:AMSRL-WM-MB
Aberdeen Proving Ground, MD 21005-5066
USA

Dr. Alan Walls
The University of Texas at Austin
Center for Electromechanics
PRC/EME, Mail Code R7000
Austin, TX 78712
USA

Mr. Norm Wells
LMMFC
P.O. Box 650003
M/S SP-97
Dallas, TX 75265-0003
USA

Mr. Michael Werst
Center for Electromechanics
The University of Texas at Austin
PRC/EME, Mail Code R7000
Austin, TX 78712
USA

Mr. Timothy Wolfe
Maxwell Technologies, Incorporated
9210 Sky Park Court
San Diego, CA 92123
USA

Mr. Alexander Zielinski
U.S. Army Research Laboratory (ARL)
AMSRL-WM-BC / B390
Aberdeen Proving Ground, MD 21005-5066
USA

Dr. Raymond Zowarka
Center for Electromechanics
The University of Texas at Austin
PRC, Mail Code R7000
Austin, TX 78712
USA